

# HYDRODYNAMIC MODEL FOR A $\beta$ Cephei VARIABLE BW Vulpeculae

A. Fokin<sup>1</sup>, Ph. Mathias<sup>2</sup>, E. Chapellier<sup>3</sup>, D. Gillet<sup>4</sup> and N. Nardetto<sup>5</sup>

<sup>1</sup> Institute of Astronomy of the Russian Academy of Sciences,  
48 Pjatnitskaya Str., Moscow 109017 Russia, *fokin@inasan.ru*

<sup>2</sup> Observatoire de la Côte d’Azur, Dpt. Gemini, UMR 6203,  
F-06304 Nice Cedex 4, *mathias@obs-nice.fr*

<sup>3</sup> Observatoire de la Côte d’Azur, Dpt. Gemini, UMR 6203,  
F-06304 Nice Cedex 4, *chapellier@obs-nice.fr*

<sup>4</sup> Observatoire de Haute Provence, CNRS, F-04870,  
Saint Michel l’Observatoire, France, *gillet@obs-hp.fr*

<sup>5</sup> Observatoire de la Côte d’Azur, Dpt. Gemini, UMR 6203,  
F-06304 Nice Cedex 4, *nardetto@obs-nice.fr*

**ABSTRACT.** A hydrodynamical model for the high-amplitude  $\beta$  Cephei star BW Vulpeculae is generated, and the spectral line profiles are calculated for different pulsational phases. The pulsational characteristics and line profiles are compared with recent observational data obtained during seven consecutive nights in August 2000. We found a generally good agreement in the basic photometric and spectral parameters. Two strong shock waves appear during one period, and the "stillstand" is due to the gas dynamics between the passages of these shocks. Note that this good agreement suppose a metallicity  $Z = 0.03$ , while a metallicity  $Z = 0.02$  does not lead to the correct amplitudes and shapes of the curves.

**Key words:** Line: profiles, stars: oscillations, stars: variable: general, stars: individuals: BW Vulpeculae

## 1. Introduction

Among the  $\beta$  Cephei stars, BW Vulpeculae (HD 199140, B2 III) exhibit the most extreme variability of light, radial velocity and line profiles. With a period of 0.201 days, the peak-to-peak amplitude of the radial velocity variation amounts to more than  $2K = 200$  km/s, the total range of the light variation is approximately 0.2 mag in  $V$ , and, finally, the spectra show well-marked line-doubling. A prominent feature of both the radial velocity curve and the light curve is the presence of a bump. This bump occurs around pulsation phase  $\varphi = 0.8$  in the light curve, whereas it occurs at pulsation phase  $\varphi = 1.0$  in the ra-

dial velocity variation and is usually called "stillstand". On each side of the stillstand, the velocity curve shows discontinuities due to line-doubling phenomena.

The interpretation of these unusual observational phenomena in a  $\beta$  Cephei star is not clear yet. Up to now, the only one attempt to model the observations was performed by Moskalik & Buchler (1994). They used a nonlinear pulsation model where the dynamics was governed by the unique outward propagating shock originating at the bottom of the HeII ionization zone. In this view, the consecutive strong compression provokes a sudden jump of the Rosseland-mean opacity which contributes to the formation of an apparent discontinuity in the observed radial velocities. However, this results in a stillstand which is at a value of about -100 km/s in the rest frame of the star, whereas its observed value is around the stellar  $\gamma$ -velocity at -9.2 km/s (MGFC).

Our main objective was to interpret observations of BW Vulpeculae using an auto-coherent pulsation model which has already been successfully used for different classes of radial pulsators, from RR Lyrae (Fokin & Gillet 1997) to RV Tauri (Fokin 2000) and post-AGB (Jeannin et al. 1997).

## 2. Observations

Spectra were obtained at the Observatoire de Haute-Provence with the 1.52 m telescope using the AURELIE spectrograph during 7 consecutive nights, from August 14 to 21, 2000. The spectral resolution was

around 25 000 along a  $120 \text{ \AA}$  spectral range centered on the SiIII triplet at 4552, 4567 and  $4574 \text{ \AA}$ . This relatively low spectral resolution allowed a very good temporal sampling: with a mean exposure time around 2 min, more than 100 spectra per pulsation period were obtained. The measured signal-to-noise is between 100 and 150. Reductions were performed using the standard IRAF package.

Since we have no simultaneous photometric observations, dates of maximum luminosity were computed following the most recent ephemeris provided by Horvath et al. (1998). Because this ephemeris gives dates concerning light minima, we added 0.1116 d (0.555 P) to retrieve the usual phase convention (Sterken et al. 1987).

### 3. Nonlinear model

The basic stellar parameters for BW Vul are still uncertain. According to different authors, the mass vary from 11 to  $14 M_{\odot}$ , luminosity from  $\log L/L_{\odot} = 4.146$  to 4.431 and  $\log T_{eff}$  from 4.33 to 4.386 (Aerts et al. 1998; Lesh & Aizenman 1978; Heynderickx 1992; Moskalik & Buchler 1994). We tried different sets of parameters, and finally have chosen a model close to the second turn-over point on the  $11 M_{\odot}$  evolutionary track of Dziembowski & Pamyatnykh (1993). The parameters of this 150-zone model are:  $M = 11 M_{\odot}$ ,  $\log L = 4.176$ ,  $\log T_{eff} = 4.362$ .

Our model was calculated with the radiative Lagrangian code by Fokin (1990). The inner boundary has been fixed to  $T = 4.4 \cdot 10^7 \text{ K}$ , corresponding to about 5% of the photometric radius and the envelope contained 83% of the stellar mass. We used the OPAL92 opacity tables, and studied both  $Z = 0.02$  and 0.03 metallicity.

The model with  $Z = 0.02$  (the metallicity used by Moskalik & Buchler (1994) reached its fundamental limit cycle with the period of 0.211 days and bolometric and radial velocity amplitudes  $\Delta m = 0.15 \text{ mag}$  and  $2K = 40 \text{ km/s}$ , respectively. Relative radial amplitude at the surface is  $\Delta R/R = 2.5\%$ . Its pulsation is sinusoidal and represents a typical  $\beta$  Cepheid star having very small amplitude, and has little in common with BW Vul.

The model with  $Z = 0.03$ , on the contrary, has reached the limit cycle with very large amplitudes,  $\Delta m_{bol} = 0.7 \text{ mag}$  and  $2K = 260 \text{ km/s}$ , with the period  $P = 0.217 \text{ days}$ . The relative radial amplitude at the surface is  $\Delta R/R = 12\%$ . This model is presented in Fig.1 where one can clearly see the bump of the light curve at phase 0.8, as well as complicate motions in high atmosphere with shock waves. According to Barry et al. (1984), the estimated bolometric magnitude should be about 0.75 mag, which is close to our theoretical value of 0.7 mag.

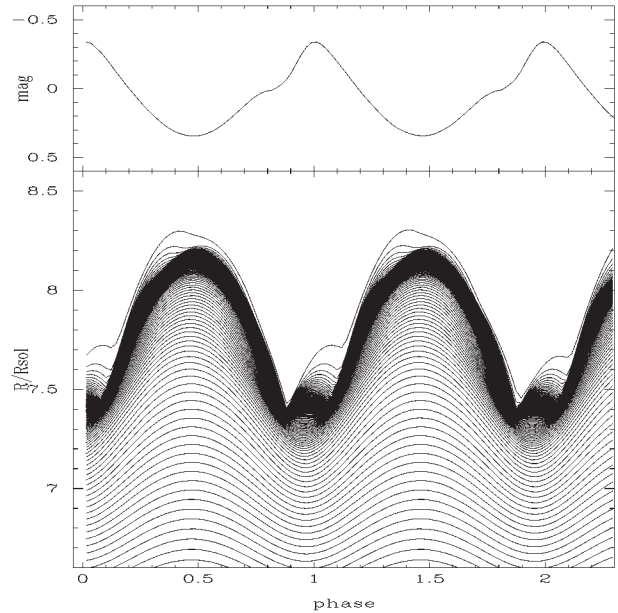


Figure 1: Theoretical bolometric light curve (upper diagram) and displacement of different mass zones (lower panel) for a BW Vul model with  $M = 11 M_{\odot}$ ,  $\log L/L_{\odot} = 4.176$ ,  $\log T_{eff} = 4.362$  and  $Z = 0.03$

The amplitude and the character of pulsation are not sensible to small variations of  $L$ ,  $T_{eff}$  and  $M$ . All these models have the characteristic bump on their light curves and a stillstand on the velocity curves. We found that the bump and the stillstand are the results of a passage of **two strong shocks** formed closely to the region of instability ( $T \approx 2.5 \cdot 10^5 \text{ K}$ ). The LNA analysis reveals that there is no low-mode resonance in the BW Vul model up to the third overtone, so the Cepheid-like explanation of the bump is not relevant.

### 4. Nature of the two shocks

The two shocks can be followed as maxima of compression rate for the most important compression/shock waves versus the mass zone in Fig.2. We also indicated the position of the zone  $T = 250 000 \text{ K}$  where the Z-peak  $\kappa$ -mechanism acts, the photosphere and both boundaries of the He ionization zone. We remark that the outer boundary of the He ionization zone (at about  $T = 40 000 \text{ K}$ ) remains strangely flat during the phase of "stillstand" between the two shock waves (Fig. 5).

After  $\varphi = 0.1$  the atmospheric expansion slows down and after the phase 0.45 turns to contraction with almost constant deceleration,  $\approx 13 \text{ m s}^{-2}$ , which is about 4 times less than the mean gravity in the model atmosphere. During the contraction phase, the compression of the gas is not homogeneous.

In the same time the luminosity from the inner zones

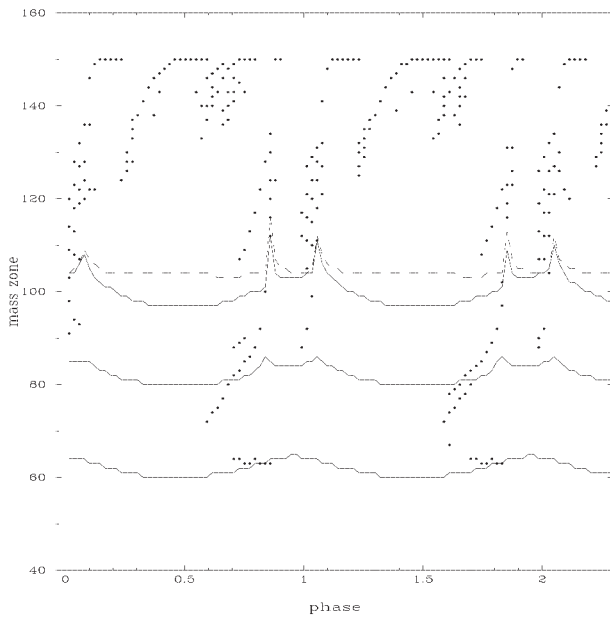


Figure 2: Shock propagation through the mass grid. Points mark the maxima of compression corresponding to the most important compression/shock waves. Solid curve below corresponds to  $T = 250\,000\text{K}$ . Two upper solid curves limit the He ionization region. The dashed curve indicates the photospheric level

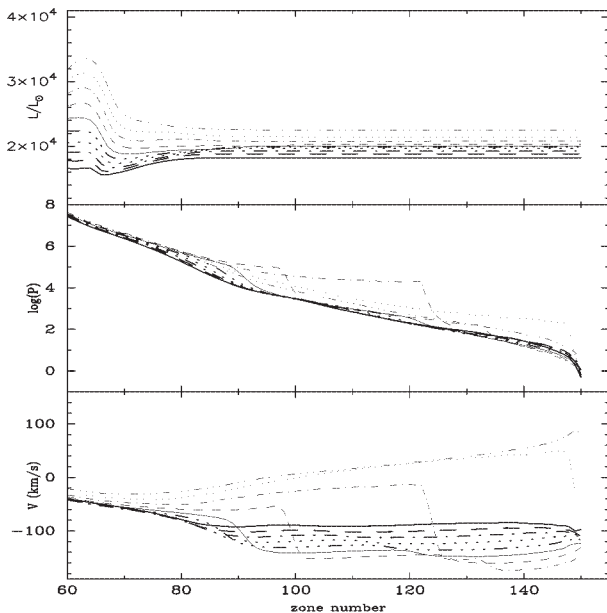


Figure 3: Time evolution of the profiles of luminosity (upper diagram), gas pressure (middle) and velocity (bottom) versus the number of the mass zone between the phases 0.69–0.87, corresponding to the generation of the shock 1. Phase 0.69 refers to the thick solid curve, and phase 0.87 - to the thin three-dotted curve. The mass zone number 60 approximately corresponds to  $T=250\,000\text{K}$ , while the mass zone 150 corresponds to the surface

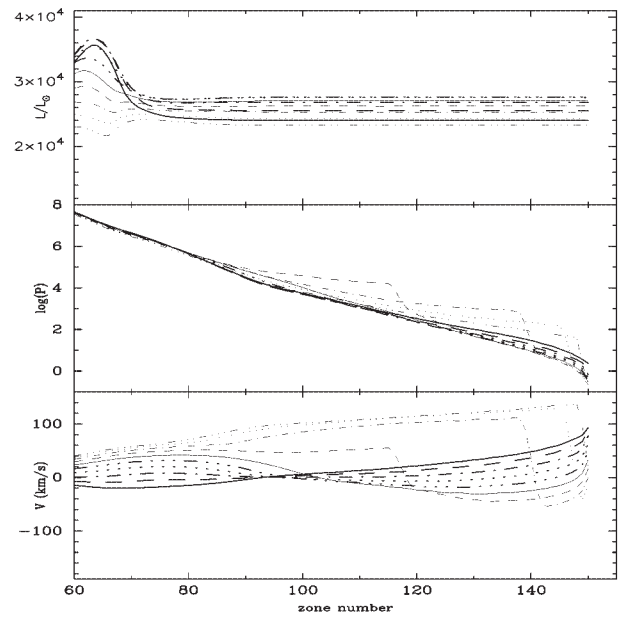


Figure 4: Same as in Fig. 3 for the phases 0.91–1.09, corresponding to the generation of the shock 2

starts rapidly increasing, but the radiation is effectively absorbed in the outer region of the Z-peak zone ( $T = 200\,000\text{K}$ ). From the phase 0.8 (the beginning of the "stillstand") until 0.95 this absorption is especially strong (see Figs. 3–4). This absorption creates an over-pressure above the Z-peak zone. After approximately the phase 0.75 the compression wave, provoked by this over-pressure, starts propagating outwards and shortly transforms into shock 1 (Fig. 3).

This shock enters the zone of He ionization, where it causes perturbations of temperature and density and, consequently, the increase of the opacity by a factor of 2. The strong radiative absorption in the region of the Z-peak and in the wake of the shock 1 is the cause of the observed bump in the light curve.

The shock 1 then increases in amplitude, up to  $140\text{ km/s}$ , and reaches a compression rate of about 100. It rapidly passes through the atmosphere and escapes. After the escape of the shock 1 the outer envelope starts expanding, while the inner shells are still in compression. The expansion of the outer atmosphere is slow. The absorption in the Z-peak region is still about  $11\,000L_{\odot}$ , but the luminosity from the inner region increases, so the total stellar luminosity starts increasing after the short bump. The accumulation of the thermal energy due to absorption in this zone continues. Near the phase 0.95 the compression starts expanding from the inner zones upwards (see Fig. 4) and a new shock 2 is formed in the helium ionization zone. At  $\phi=1.1$  it arrives to the surface and escapes.

An important result from the above analysis is that both shock waves have origin in the region laying well below the photosphere and are due to the  $\kappa$ -mechanism

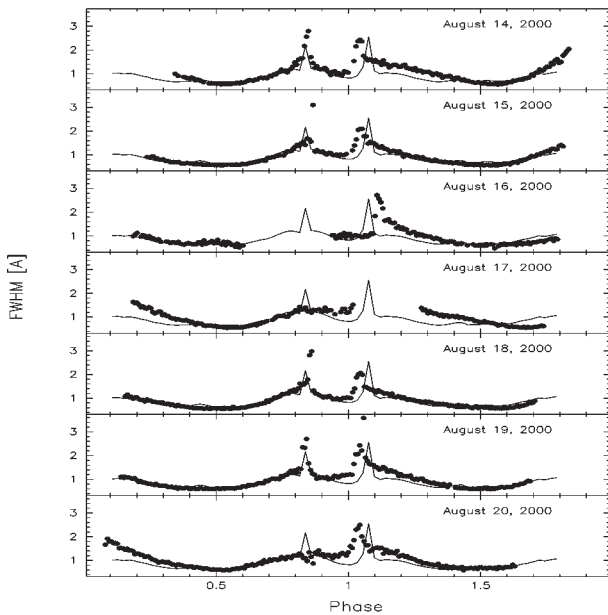


Figure 5: Theoretical (solid) and observational (points) FWHM of the Si III 4553 Å line. The comparison is presented for all seven consecutive nights, with the dates indicated in each diagram

in the Z-peak zone.

### 5. Line profiles: theory and observations

After the model has been generated, we calculated a series of snap-shots of the atmospheric structure (about 50 per pulsational period) in order to study the theoretical line profiles. The line transfer problem for each model atmosphere was resolved with the code of Fokin (1991) under the LTE assumption. For all phases we assume the same microturbulent velocity of 1 km/s, and we considered a projected rotation velocity of  $v \sin i = 24$  km/s (Stankov et al. 2003).

In Figs. 5-6 we present the detailed comparison of different features of the predicted profiles versus the observational ones obtained in 7 consecutive nights in August 2000. Note that the theoretical curve is the same in each diagram, and is compared with the observed curves for different nights. These diagrams show, respectively, the FWHM (Fig. 5) and the radial velocities measured at the minima of the principal absorption components (Fig. 6).

Note that the observational curves are noticeably variable from cycle to cycle. If we fix some phases, we shall see that the discrepancy between the observed and predicted curves as well significantly varies from night to night. This behaviour cannot be explained by our model, because it is strictly periodic.

The radial velocity curves (Fig. 6) show very good agreement with the observations for almost all the

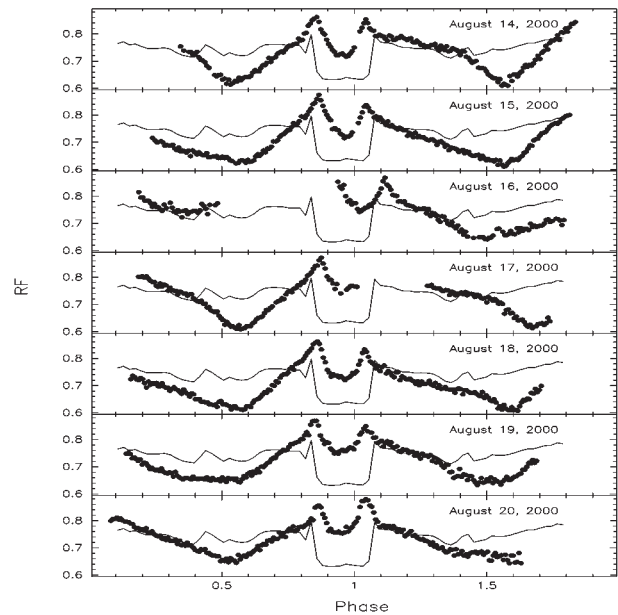


Figure 6: Same as in Fig. 5 for the radial velocities measured from the minima of the principal absorption component

nights. We note that the "stillstand" is rather an idealization, especially clearly seen in the curve of August 16: during this period the velocity varies significantly, a fact confirmed by our model.

Generally, the comparison is good and confirms the consistence of our model.

### 6. Conclusion

Our nonlinear model represents reasonably well the observed features of BW Vulpeculae. Two shocks are generated consequently - one at each phase of the observed velocity discontinuities, and not only one as previously stated by Moskalik and Buchler (1994)). The physical origin of these shocks is suggested to be a strong radiative absorption in the zone of the "Z-peak". Also, the characteristic asynchronous motions of the upper and lower envelope regions can contribute to the shock generation. We stress that both shocks are generated below the photosphere.

We found that a metallicity  $Z = 0.02$  is too low, so that the observed amplitudes can be reproduced only with  $Z = 0.03$ . The linear analysis shows that the only driving zone in the models is that of the "Z-peak" of opacity at  $\log T = 5.2 - 5.4$ . Just above and below there are two regions of positive dissipation. LNA calculations show that the model with  $Z = 0.03$  is unstable in the F-mode, while the  $Z = 0.02$  model is only marginally unstable. We found that the lower damping zone becomes more effective as  $Z$  decreases from 0.03 to 0.02 which possibly explains lower amplitude

for  $Z=0.02$ . We suggest that other members of the  $\beta$  Cepheid group, having much smaller amplitudes than BW Vul, probably have lower metallicity, as shown in our second model, identical except for  $Z = 0.02$ .

### References

- Aerts C., Mathias P., Van Hoolst T. et al.: 1995, *A&A*, **301**, 781.
- Barry D.C., Holberg J.B., Forrester W.T. et al.: 1984, *ApJ*, **281**, 766.
- Dziembowski W.A., Pamiatnykh A.A.: 1993, *MNRAS*, **262**, 204.
- Fokin A.B.: 1990, *ApSS*, **164**, 95.
- Fokin A.B.: 1991, *MNRAS*, **250**, 258.
- Fokin A.B., Gillet D.: 1997, *A&A*, **325**, 1013.
- Fokin A.B.: 2001, *In Stellar pulsation - nonlinear studies, ASSL series, ed. by M.Takeuti and D.D.Sasselov*, **257**, 103-136.
- Heynderickx D.: 1992, *PhD thesis, Katholieke Universiteit Leuven, Belgium*.
- Horvath A. Gherega O. Farkas L.: 1998, *Rom. Astron. Journal*, **8**, 89.
- Jeannin L., Fokin A.B., Gillet D., Baraffe I.: 1997, *A&A*, **326**, 203.
- Lesh J.R., Aizenman M.L.: 1978, *ARA&A*, **16**, 215.
- Moskalik P., Buchler J.R.: 1994, *in: L.A. Balona, H.F. Henrichs & J.-M. Le Contel (Eds) Pulsation, Rotation and Mass Loss en Early-Type Stars, IAU 162, Kluwer Academic Publishers, p.19*.
- Stankov A., Ilyin I., Fridlund C.V.M.: 2003, *A&A*, **408**, 1077.